IEEE Photonics Journal
An IEEE Photonics Society Publication

A WDM-PON-Compatible System for Simultaneous Distribution of Gigabit Baseband and Wireless Ultrawideband Services With Flexible Bandwidth Allocation

Volume 3, Number 1, February 2011

Tien-Thang Pham, Member, IEEE
Xianbin Yu, Member, IEEE
Timothy Braidwood Gibbon, Member, IEEE
Lars Dittmann, Member, IEEE
Idelfonso Tafur Monroy, Member, IEEE

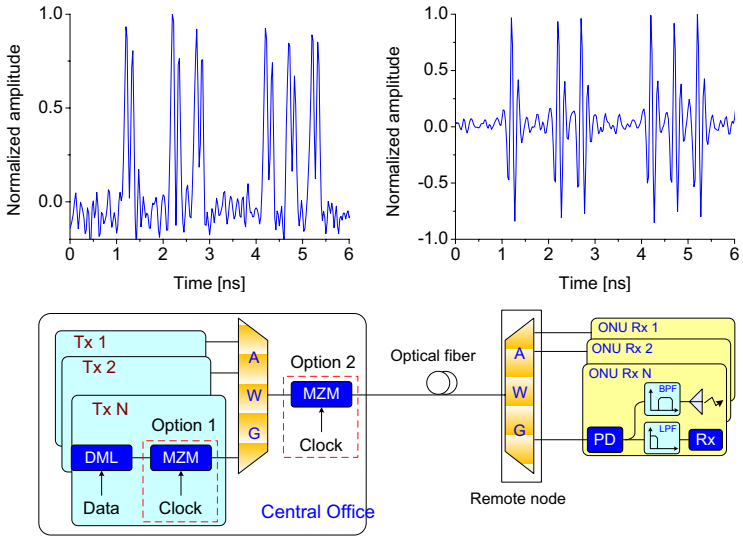

DOI: 10.1109/JPHOT.2010.2095834
1943-0655/$26.00 ©2010 IEEE

A WDM-PON-Compatible System for Simultaneous Distribution of Gigabit Baseband and Wireless Ultrawideband Services With Flexible Bandwidth Allocation

Tien-Thang Pham, *Member, IEEE*, Xianbin Yu, *Member, IEEE*, Timothy Braidwood Gibbon, *Member, IEEE*, Lars Dittmann, *Member, IEEE*, and Idelfonso Tafur Monroy, *Member, IEEE*

DTU Fotonik, Department of Photonics Engineering, Technical University of Denmark, DK-2800 Kgs. Lyngby, Denmark

DOI: 10.1109/JPHOT.2010.2095834

Manuscript received October 27, 2010; accepted November 20, 2010. Date of publication November 29, 2010; date of current version January 24, 2011. Corresponding author: T. T. Pham (e-mail: ptit@fotonik.dtu.dk).

Abstract: In this paper, a novel and simple scheme to realize flexible access for gigabit wireline and impulse radio ultrawideband (IR-UWB) wireless services is proposed. The UWB signals are generated by multi-carrier upconverting and reshaping the baseband signals. The proposed system was experimentally demonstrated with the performances of 2.0-Gb/s data in both baseband and UWB formats after 46-km single mode fiber transmission and further 0.5-m wireless for UWB data. The flexibility of the system is confirmed by investigating the system performance at different data rates including 1.0 and 1.6 Gb/s. Optical wavelength independency and data-rate variability of UWB signal generation makes the system attractive for potential wireline and wireless applications in existing wavelength division multiplexing (WDM)-passive optical network (PON) systems.

Index Terms: Microwave photonics, ultrawideband (UWB), radio over fiber, wavelength division multiplexing (WDM), passive optical network (PON).

1. Introduction

Ultrawideband (UWB) is finding its application in high-speed wireless communication systems as well as sensor applications [1]. Regulated by the U.S. Federal Communications Commission (FCC) for the spectral band from 3.1 to 10.6 GHz, the power spectral density (PSD) of a UWB transmitter is limited to -41.3 dBm/MHz [2], which is below the noise level of other wireless communication systems such as the Global Positioning System (GPS), Global System for Mobile Communications (GSM), and Worldwide Interoperability for Microwave Access (WiMAX). The low emitted PSD causes the wireless transmission distance to be limited to within a few meters. In this context, UWB-over-fiber is a promising technology for extending the coverage of UWB services. Recently, several techniques have been proposed to optically generate impulse radio UWB (IR-UWB) signals using a fiber-Bragg-grating-based frequency discriminator [4], a gain-switch laser [5], or relaxation oscillations of a laser [6].

On the other hand, passive optical networks (PONs) are highly recognized as the most promising candidates for next-generation optical access systems to satisfy the increasing bandwidth demand

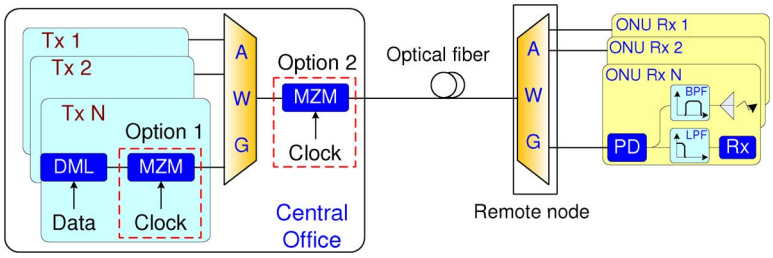

Fig. 1. Proposed WDM-PON system for photonic UWB generation and distribution. DML: directly modulated laser, MZM: Mach–Zehnder modulator, AWG: arrayed waveguide gratings, PD: photodetector, HPF: high-pass filter, LPF: low-pass filter. MZM can be used by a single channel (placed after the DML—option 1) or shared by many WDM channels (placed after the AWG—option 2) if they operate at the same data rate.

from households as well as enterprises [8]. The convergence of distributing wireline and wireless services including IR-UWB service over a common PON architecture is regarded as a potential solution to exploit cost-efficiently and, with a high degree of flexibility, the benefits of low-loss and high-bandwidth optical fiber access plants. However, to realize this vision, it is mandatory to conceive simple approaches for photonic generation of IR-UWB signals with common photonic PON components as well as to develop simple and flexible methods for service differentiation and dynamic bandwidth allocation. Recently, Pan *et al.* have demonstrated an electrically generated UWB signal that can share a single wavelength with a baseband signal in a wavelength division multiplexing-PON (WDM-PON) system [9]. The authors also have demonstrated the seamless integration of UWB service in a WDM-PON system that supports a variety of wireline and wireless services [10].

In this paper, we propose and experimentally demonstrate a novel, simple, and flexible method to generate gigabit FCC-compliant IR-UWB signals by optically upconverting baseband signals using their clock signal as a source of multiple sinusoidal signals. Assisted by a digital signal processing (DSP) receiver, the data in both the baseband and UWB formats at 1, 1.6, and 2 Gb/s are recovered without error bits after 46-km single mode fiber (SMF) and further 0.5-m wireless for the UWB signal. The fact that the baseband bandwidth for the wireline service can be shared with the wireless service just by switching on the clock signal enables flexible access connectivity for end-users with a less-complex architecture. Additionally, wavelength-independent operation makes our proposed system compatible with existing WDM-PONs.

2. Proposed System and Operation Principle

Fig. 1 depicts the proposed WDM-PON supporting UWB and wireline baseband service distribution. The operation principle of this scheme is based on the use of the same wireline baseband data source for UWB service. At the central office (CO), for each end-user, an electrical baseband signal drives a directly modulated laser (DML). The baseband data is then mixed with multiple optical-intensity-modulated sinusoidal signals at a Mach–Zehnder modulator (MZM). Due to the nature of the sum of sinusoidal signals at different frequencies, the clock signal is utilized to drive the MZM. The are two options for the position of the MZM, as shown in the figure. If the MZM and the clock signal is used separately by a single channel, it is placed after the DML (Option 1). Optical signals from all WDM channels are combined by an array waveguide grating (AWG). The MZM and clock signal also can be shared by several WDM channels if they operate at the same data rate (Option 2). In this case, the MZM is placed after the AWG. The combined optical signal is transmitted to an AWG-based remote node (RN) through a fiber. At the output of the photodiode (PD) of each optical network unit (ONU), there are copies of the data at both the baseband and the harmonic frequencies of the modulating sinusoidal signals. Therefore, by using appropriate electrical filtering at the ONU, both wireline baseband and FCC-compliant wireless IR-UWB signals are achieved for service distribution. This scheme provides wireless service dynamically as connectivity to the UWB service is simply enabled by switching the clock signal on or off.

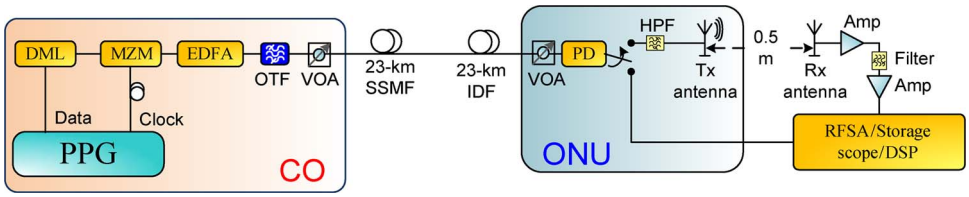

Fig. 2. Experimental setup of photonic UWB generation, distribution, and detection. DML: directly modulated laser, MZM: Mach–Zehnder modulator, PPG: pulse pattern generator, EDFA: erbium-dropped fiber amplifier, OTF: optical tunable filter, SSMF: standard single mode fiber, IDF: inverse dispersion fiber, VOA: variable optical attenuator, PD: photodetector, RFSA: radio frequency spectrum analyzer, DSP: digital signal processing, Amp: electrical amplifier. HPF: high-pass filter.

3. Experimental Setup

The experiment setup of the proposed system is shown in Fig. 2. A 4-Gb/s programmed pattern from a pulse pattern generator (PPG) was used to drive a DML. The reversed lasing threshold and bias currents of the DML were −11 mA and −31 mA, respectively. A sequence of 2 bits from the PPG was used to generate one UWB bit. Due to the negative bias of the DML, "0" and "1" UWB bits are represented by the sequences of "11" and "10," respectively. The data from the PPG is thus 50% inverted return-to-zero (RZ), and the effective bit rate of the UWB signal is 2 Gb/s. The output of the DML was then launched into a 10-GHz MZM. The clock signal from the PPG at 4 Gb/s was used as a multiple-subcarrier source to drive the MZM. The MZM biased at 3 V operated at a nonlinear region to modify the amplitude of subcarriers and consequently shape the waveform of the generated UWB signal. An Erbium-dropped fiber amplifier (EDFA) and a tunable optical filter (TOF) with 0.9-nm 3-dB bandwidth were employed to amplify the optical signal and reject out-band amplified spontaneous emission (ASE) noise. The optical signal was transmitted over a 46-km link including 23-km standard SMF and dispersion-matched 23-km inverse dispersion fiber (IDF) and then detected by a PD with 12-GHz bandwidth. The losses of SMF and IDF fibers were 5.1 dB and 7.7 dB, respectively. The detected signal was filtered by a commercially available high-pass filter (HPF) with 3.1-GHz cutoff frequency to form UWB pulses. The detected signal was also used to recover the transmitted data in the baseband. The UWB signal was radiated into the free space by an Omni-directional antenna (Skycross SMT-3TO10M-A). The wireless transmission distance was set at 0.5 m. The radiated UWB signal was received by a directive antenna (Geozondas AU-3.1G10.6G-1). Data in both the UWB and baseband formats were sampled, stored at 40 GSa/s by a digital sampling scope (DSO Agilent Infiniium 8000B), and then processed offline by using a DSP receiver.

4. Experimental Results and Discussions

Fig. 3(a) and (b) illustrate the electrical spectra of the UWB signals with a $2^7 - 1$ pseudorandom binary sequence (PRBS) pattern length after 46-km fiber transmission at −19 dBm received optical power with and without the HPF. The effective mask is the allowed mask when the frequency response of the transmitting antenna is taken into account [3]. As shown in the figure, the obtained UWB signals were fully compliant with the FCC mask. Fig. 3(c) and (d) show the detected electrical spectra when the clock signal and data were off, respectively. When the clock signal was off, some frequency components (<-50 dBm/MHz) could be observed in the UWB frequency band, which was caused by the relaxation oscillations of the DML operating close to the threshold current. When the clock signal was applied to the MZM, PSD at high-frequency band increased over 10 dB, and the generated UWB signal met the FCC requirements from 3.1 to 10.6 GHz. Fig. 4(a) and (b) show the detected waveform of the sequence "001011001110" before and after the HPF. We can notice that the waveform of the generated UWB pulse is similar to a fifth-order Gaussian derivative, which is known to agree well with the FCC spectra requirements for UWB systems [6]. Fig. 4(c) illustrates the waveform of the received UWB signal after wireless transmission.

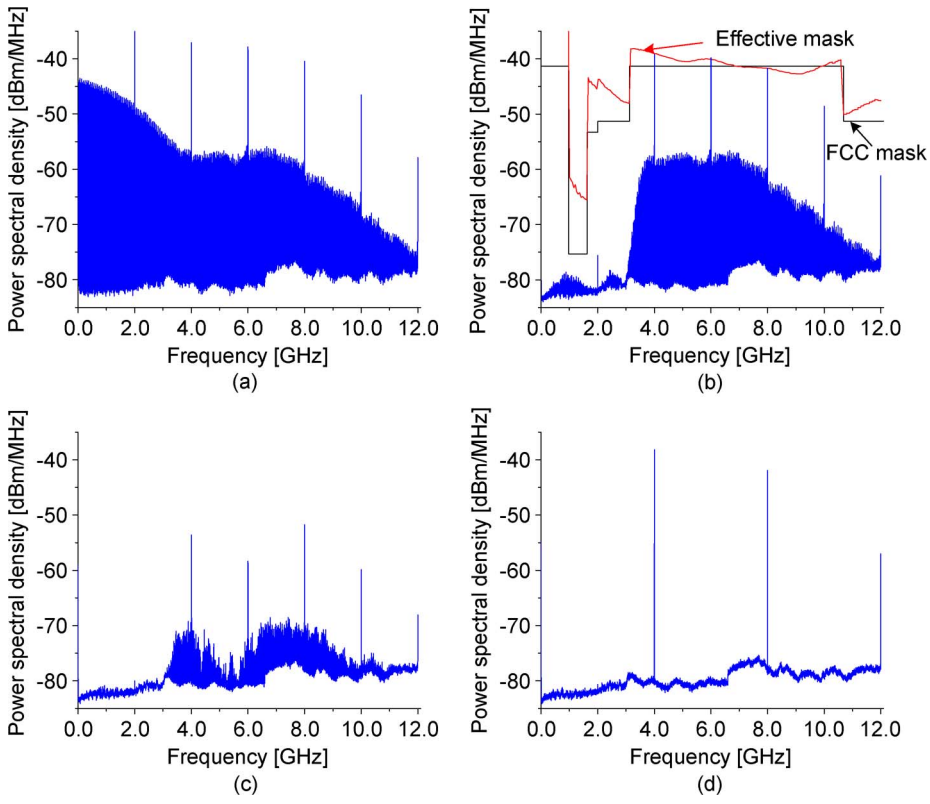

Fig. 3. Electrical spectra of detected 2-Gb/s baseband and UWB signals at −19 dBm after fiber transmission. (a) Without the HPF, (b) with the HPF, (c) with the HPF and clock off, and (d) with the HPF and data off.

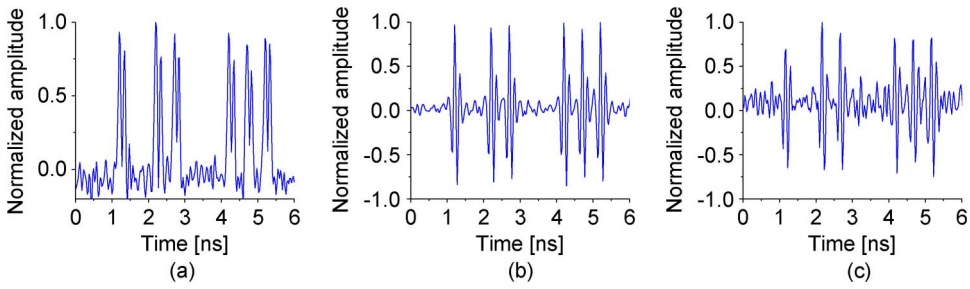

Fig. 4. Waveforms of the pattern "001011001110" at 2 Gb/s (a) without the filter, (b) with the filter (inside the mask), and (c) after 0.5-m wireless transmission.

4.1. Performance of 2-Gbps UWB Signal

To assess the performance of the UWB signal, 100 000 UWB bits were recorded and processed offline using a DSP algorithm. The DSP comprises of noise filtering, bit correlation, and threshold detection functions [7]. In the final step, value of each detected UWB bit was determined by comparing the sum of some sampled points within each bit slot to an optimally determined decision threshold. The measured bit-error-rate (BER) curves of the UWB data at back-to-back (B2B), after 46-km fiber transmission, and 0.5-m wireless transmission are shown in Fig. 5(a). Without wireless transmission, errors appeared when optical power was −25 dBm. The inset is the eye-diagram of the UWB signal at this optical power after 46-km fiber. There was no power penalty after fiber transmission as the dispersion induced by the SMF was completely compensated by the IDF. After

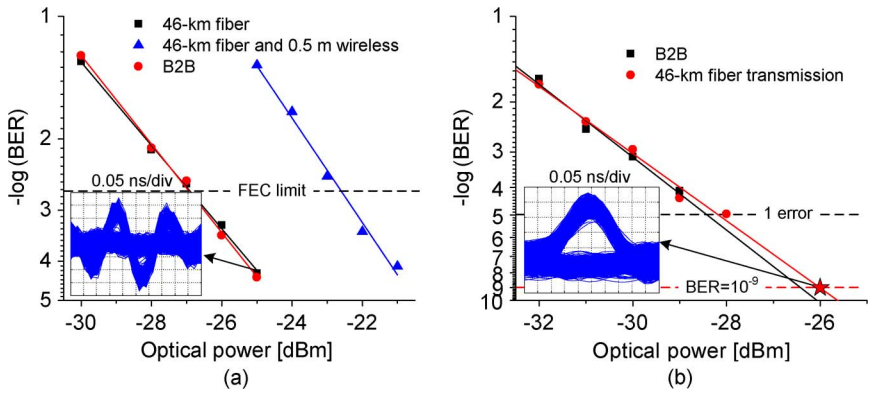

Fig. 5. Transmission performance of both 2-Gb/s data in (a) UWB and (b) baseband formats.

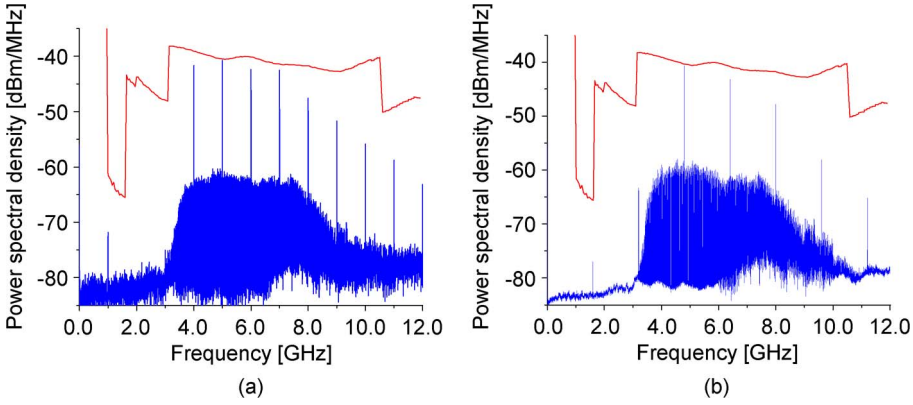

Fig. 6. Electrical spectra of detected (a) 1.0-Gb/s data and (b) 1.6-Gb/s UWB signals after fiber transmission.

wireless transmission, errors were recorded at -21 dBm. The received optical power to achieved the forward error correction (FEC) limit $(\mathrm{BER} = 2 \times 10^{-3})$ was approximately -22.7 dBm. Therefore, at this BER requirement, 0.5-m wireless transmission introduced about a 4.5-dB power penalty.

4.2. Performance of 2-Gb/s Baseband Signal

For the baseband data, the corresponding DSP algorithm includes low-pass filtering and threshold decision functions to demodulate the received signal. The cutoff frequency of the digital low-pass filter was 4 GHz. Unlike the UWB data, the logic value of each bit was determined by comparing the value at only one sampled point to an optimally determined decision threshold. This process emulated a conventional receiver. The measured BER curves of 100 000-bit baseband data with and without fiber transmission are also shown in Fig. 5(b). Similar to the performance of the UWB signal, there was no power penalty after 46-km fiber transmission. The required optical power to achieve the same BER for the baseband signals was about 4 dB lower than for the UWB signals without wireless transmission, because the baseband signals had higher signal-to-noise ratio (SNR), as shown in Fig. 3(a). Moreover, by extrapolating the linearized BER curves, $\mathrm{BER} < 10^{-9}$ of the baseband can be approximately achieved at -26 dBm for both B2B and fiber transmission, which is compatible with existing WDM-PON systems. The inset displays the eye-diagram of the baseband data at -26 dBm.

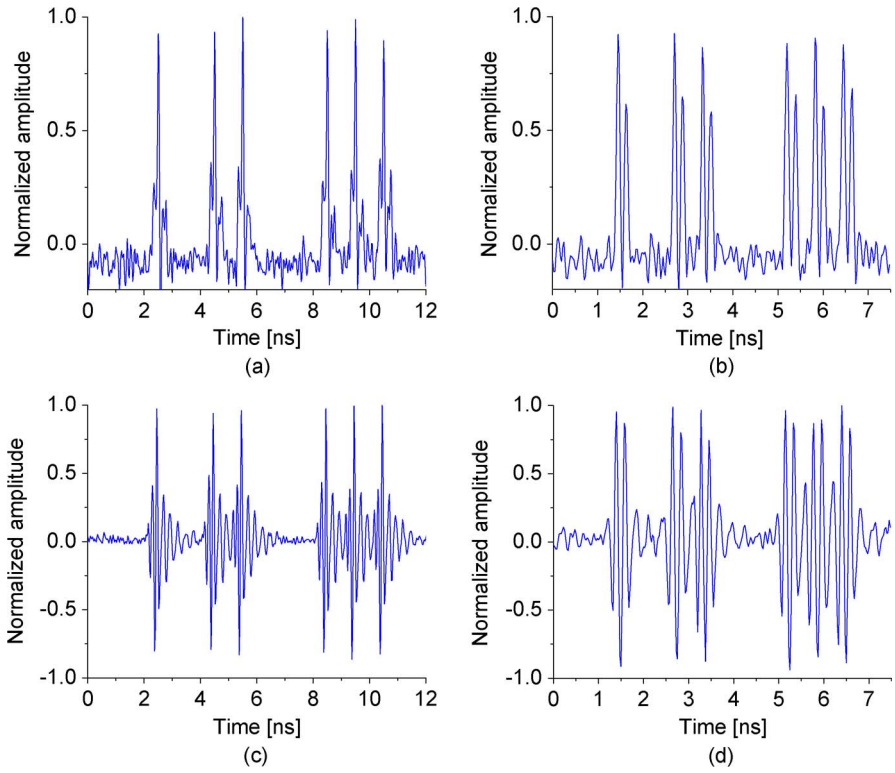

Fig. 7. Waveforms of the pattern "001011001110" at (a) 1.0 Gb/s and (b) 1.6 Gb/s without the HPF (Baseband), (c) 1.0 Gb/s and (d) 1.6 Gb/s with the HPF (UWB).

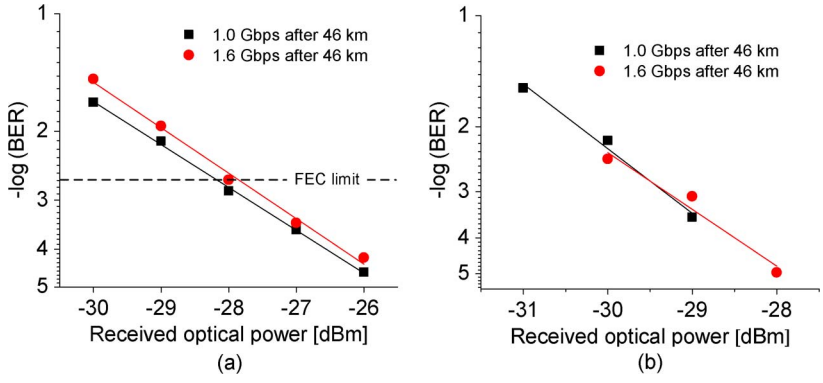

Fig. 8. Transmission performance of both 1.0-Gb/s and 1.6-Gb/s data in (a) UWB and (b) baseband formats.

4.3. Flexible Data-Rate Allocation

To investigate the data-rate flexibility of our proposed method, we varied the frequency of the PPG to 3.2 GHz and 2 GHz with no other changes of the setup, and thus, the data rates of both the baseband and UWB signals were lowered to 1.6 and 1.0 Gb/s. The maximum received optical powers to fit the FCC mask were approximately −20 dBm for both 1.6- and 1.0-Gb/s data. The electrical spectra of detected UWB signals at this optical power level are shown in Fig. 6. The corespondent waveforms of the sequence "001011001110" at these bit rates with and without HPF are displayed in Fig. 7. The transmission performances of both the baseband and UWB signals are illustrated in Fig. 8. Compared with the 2-Gb/s case, the baseband signals had similar performance.

However, the sensitivities of the 1.6-Gb/s and 1.0-Gb/s UWB signals at BER of $< 2 \times 10^{-3}$ were about 1.0 and 1.3 dB better, respectively, because they required received optical power to fit the mask about 1 dB lower than the 2-Gb/s case. Longer wireless transmission distances for the UWB signals at these bit rates can be achieved at the same received optical power and BER requirement.

5. Conclusion

A simple system supporting flexible gigabit wireline and IR-UWB wireless access for IR-UWB-over-fiber based on multi-subcarrier upconversion has been proposed and experimentally demonstrated. The same wireline baseband data is used for the UWB service. The FCC-compliant UWB signals were generated by multi-carrier upconverting and reshaping the baseband signals. This method offers very simple UWB generation and efficiently improves access flexibility. Both wireline and UWB wireless connectivity to end-users can be easily realized using a common PON component and fiber plant. The performance of the proposed system was evaluated by the BER of both the wireline baseband and wireless UWB signals. Additionally, optical wavelength independency and data-rate flexibility of UWB signal generation makes the system compatible with existing WDM-PON systems.

References

[1] D. Porcino and W. Hirt, "Ultra-wideband radio technology: Potential and challenges ahead," *IEEE Commun. Mag.*, vol. 41, no. 7, pp. 66–74, Jul. 2003.
[2] Fed. Commun. Comm., *Revision of Part 15 of the Commission's Rules Regarding Ultra-Wideband Transmission Systems*, 2002.
[3] M. Abtahi, M. Mirshafiei, S. LaRochelle, and L. A. Rusch, "All-optical 500-Mb/s UWB transceiver: An experimental demonstration," *J. Lightw. Technol.*, vol. 26, no. 15, pp. 2795–2802, Aug. 2008.
[4] F. Zeng and J. Yao, "Ultrawideband impulse radio signal generation using a high-speed electrooptic phase modulator and a fiber-Bragg-grating-based frequency discriminator," *IEEE Photon. Technol. Lett.*, vol. 18, no. 19, pp. 2062–2064, Oct. 2006.
[5] A. Kaszubowska-Anandarajah, P. Perry, L. P. Barry, and H. Shams, "An IR-UWB photonic distribution system," *IEEE Photon. Technol. Lett.*, vol. 20, no. 22, pp. 1884–1886, Nov. 2008.
[6] X. Yu, T. B. Gibbon, M. Pawlik, S. Blaaberg, and I. T. Monroy, "A photonic ultra-wideband pulse generator based on relaxation oscillations of a semiconductor laser," *Opt. Express*, vol. 17, no. 12, pp. 9680–9687, Jun. 2009.
[7] T. B. Gibbon, X. Yu, and I. T. Monroy, "Photonic ultra-wideband 781.25 Mbit/s signal generation and transmission incorporating digital signal processing detection," *IEEE Photon. Technol. Lett.*, vol. 21, no. 15, pp. 1060–1062, Aug. 2009.
[8] G. K. Chang, A. Chowdhury, Z. Jia, H. C. Chien, M. F. Huang, J. Yu, and G. Ellinas, "Key technologies of WDM-PON for future converged optical broadband access networks," *IEEE/OSA J. Opt. Commun. Netw.*, vol. 1, no. 4, pp. C35–C50, Sep. 2009.
[9] S. Pan and J. Yao, "Simultaneous provision of UWB and wired services in a WDM-PON network using a centralized light source," *IEEE Photon. J.*, vol. 2, no. 5, pp. 712–718, Oct. 2010.
[10] K. Prince, J. B. Jensen, A. Caballero, X. Yu, T. B. Gibbon, D. Zibar, N. Guerrero, A. V. Osadchiy, and I. T. Monroy, "Converged wireline and wireless access over a 78-km deployed fiber long-reach WDM PON," *IEEE Photon. Technol. Lett.*, vol. 21, no. 17, pp. 1274–1276, Sep. 2009.